DYNAMIC RESPONSE ANALYSIS OF A CANTILEVER BEAM SUBJECTED TO BASE EXCITATION

[1]Amit Pradip Pharande
[1]PG Student
[1]Mechanical Design Engineering
[1]Walchand College of Engineering, Sangli, India.

Abstract: This paper is related to cantilever beam subjected to base excitation. The mathematical model of the cantilever beam under sinusoidal base excitation is prepared. Then governing differential equation and its solution for this system is obtained. With the help of MATLAB software dynamic response curves and mode shapes are obtained. The effect of internal damping and external damping on the dynamic response is analyzed. The effect of variation of beam dimensions as well as beam material on the dynamic response is analyzed. The dynamic response of the equivalent cantilever beam with fixed base and applied external excitation force is obtained and compared with the base excitation system.

I. INTRODUCTION

The engineering structures such as bed of the machine tool, beams, shafts, axles, frames etc., possess mass and elasticity. When such structures are excited by the dynamic loads they vibrate. These structures are continuous systems and have more than one natural frequency. If any one of the excitation frequencies coincides with any one of the natural frequency of the continuous system, the resonance takes place. The resonant amplitude is very large which may produce large deflection of the structure giving rise to very high induced stresses causing failure of the structure, if these stresses are beyond the allowable stress. Many of such structures shown in fig. 1.1 may be modelled as cantilever beams. As such, it is necessary to analyze the dynamic response of cantilever type structures, at design stage, subjected to harmonic base excitation. In the literature, the results of dynamic analysis of cantilever type structures subjected to force excitation are reported. Very few results on dynamic response analysis of cantilever type structures subjected to base (kinematic) excitation have been reported in the literature. As such in this dissertation work, it is proposed to carry out the dynamic response analysis of a cantilever beam type structure subjected to harmonic base excitation. Many real life applications (tall vertical buildings, watch towers, chimneys, electric transmission towers, wind mill supporting pole, airplane wings etc.) cantilever type structures are subjected to base excitation.

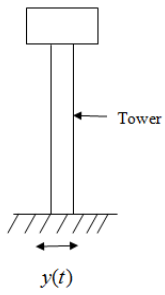

(a) Tower

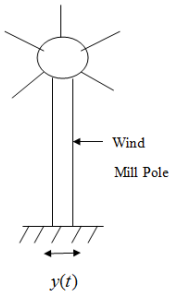

(b) Wind mill pole

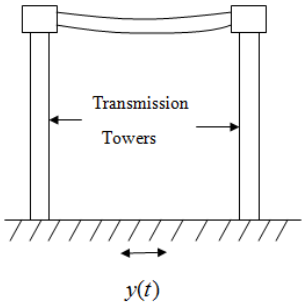

(c) Transmission tower

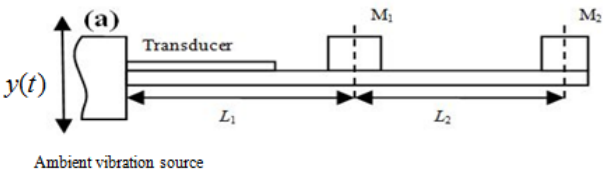

(d) 2DOF Piezoelectric vibration harvester [8]

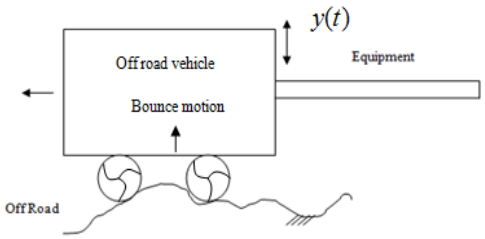

(e) Off-road vehicle equipment

Fig.1.1. Structures subjected to base excitation

Figure 1.2 shows a typical cantilever beam of length (l), width (b), and thickness (t). (b>>t) subjected to base (kinematic or motion) excitation.

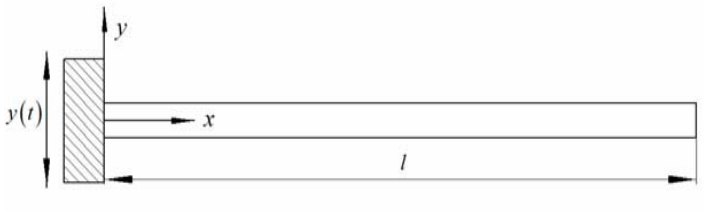

Fig.1.2. Cantilever beam under harmonic base excitation [7]

The equation of motion of cantilever beam system shown in fig.1.2 will be analyzed using classical Euler-Bernoulli beam theory and its dynamic response will be obtained using the modal superposition method and the natural frequencies and mode shapes of this system will be determined.

II. LITERATURE REVIEW

Researchers in the past have carried out some theoretical and experimental studies in the area of dynamic response analysis of cantilever beam type structures subjected to force excitation. It is seen that, very few research results are available on the cantilever beam type structures subjected to base excitation. Some of the important research results in this area reported in literature are reviewed briefly.

Freundlich2018 [1]*has carried out the transient vibrations analysis of a Bernoulli-Euler cantilever beam with a rigid mass attached at the end and subjected to base motion. The viscoelastic properties of the beam material are described using a fractional Kelvin-Voigt model. The Riemanne-Liouville fractional derivative of an order of 0 <gamma <1 is used. Exact relationships for the natural frequencies and mode shapes of the beam are derived. Moreover, a method of calculating the damped natural frequencies of the analyzed beam is presented. The forced-vibration solution of the beam is derived using the mode superposition method. Transient movement of the base is described by an oscillating function with a linearly time-varying frequency. A convolution integral of the fractional Green's and forcing functions is used to achieve the beam response.

Meesala2018 [2] has modeled the nonlinear dynamics of a cantilever beam with tip mass system subjected to different excitation and exploited the nonlinear behavior to perform sensitivity analysis and propose a parameter identification scheme for nonlinear piezoelectric coefficients. A governing equation of a cantilever beam with a tip mass subjected to principal parametric excitation has been developed by using Generalized Hamilton's Principle taking into consideration the nonlinear boundary conditions. Using a Galerkin's discretization scheme, the discretized equation for the first mode is developed for simpler representation assuming linear and nonlinear boundary conditions. Distributed parameter and discretized equations separately has been solved using the method of multiple scales. Cantilever beam tip mass system subjected to parametric excitation is highly sensitive to the detuning is determined. Assuming linearized boundary conditions yields the wrong type of bifurcation has shown.

Sonawane and Talmale2017 [3] have carried out the theoretical and experimental modal analysis of single rectangular cantilever plate. To determine the natural frequency and mode shape of a single rectangular cantilever beam condition and to compare the results obtained by finite element analysis with experimental results was the main objective. Design of cantilever beam of rectangular plate and analysis in ANSYS has been carried out. A good correlation between the mathematical, FEA and experimental result is observed. The analysis result helps in depicting the failure loads for different conditions. Aluminum single rectangular cantilever plate is studied in their work. For mathematically Euler's Bernoulli's beam theory is used. The results obtained by both the methods are found to be satisfactory.

Skoblar et al. 2016 [4] have carried out the calculation of the dynamic response to harmonic transverse excitation of cantilever Euler-Bernoulli beam carrying a point mass with the mode superposition method. This method uses mode shapes and modal coordinate functions which are calculated by separation of variables and Laplace transformations. A procedure for defining natural frequencies, mode shapes and functions of modal coordinates is described and results are used in the modal superposition method. The accuracy of defined expressions is confirmed on examples with and without Rayleigh damping.

Pawar and Sawant2015 [5] have carried out the analysis of cracked cantilever beam subjected to harmonic excitation to obtain its dynamic response by considering nonlinearities present in it. In order to carryout nonlinear dynamic analysis first of all nonlinearities present in the dynamic system have been found out. The nonlinearities presenting cantilever beam are obtained by doing theoretical, numerical and experimental static analysis of cantilever beam. For numerical, static analysis ANSYS software has been used. An experimental setup for vibration analysis of cracked cantilever beam is developed and results of both are compared and verified. In this verification the results of numerical and experimental analysis are closer to each other is observed.

Kotambkar2014 [6] has investigated the mass loading effect due to accelerometer on the natural frequency of slender beam in free-free configuration. Analytical formulation to compute modal properties of a mass loaded beam has been developed. The beam is considered as Euler-Bernoulli beam with additional mass effect is modeled by considering jump in shear force at the location and modal properties are investigated. The conclusion has been made such that for validation of the geometric model before its use for further analyses, results of software based modal analysis have to agree closely with the experimental modal analysis of the physical system.

Sun et al. 2013 [7] have determined the response distributions of cantilever beam under sinusoidal base excitation. By moment and force equilibrium equations, an analytical model is built for this cantilever beam, and then a method to predict dynamic

response at base excitation is proposed. Finally, the method is used to solve the vibration response distributions of the cantilever beam at base excitation. Correctness of this method is also proved by comparing the result with experimental data.

Wu et al. 2012 [8] have developed a novel compact piezoelectric energy harvester using two vibration modes. The harvester comprises one main cantilever beam and an inner secondary cantilever beam, each of which is bonded with piezoelectric transducers. By varying the proof masses, the first two resonant frequencies of the harvester can be tuned close enough to achieve useful wide bandwidth. Experiment and simulation to validate the design concept has been carried out. The results show that the proposed novel piezoelectric energy harvester is more adaptive and functional in practical vibration circumstances.

Velazquez2007 [9] has investigated the vibration of a highly flexible cantilever beam. The order three equation of motion developed by Crespo da Silva for the nonlinear flexural-flexural-torsion vibration of in extensional beams, are used to investigate the time response of the beam subjected to harmonic excitation at the base. The equation for the planar flexural vibration of the beam is solved using the finite element method. The finite element model developed in this work employs Galerkin's weighted residuals method, combined with the Newmark technique, and an iterative process.

Banks and Inman1989 [10] have used a partial differential equation model of a cantilever beam with a tip mass at its free end to study damping in a composite. Four separate damping mechanisms consisting of air damping, strain rate damping, spatial hysteresis and time hysteresis are considered experimentally. Dynamic tests were performed to produce time histories. The time history data is then used along with an approximate model to form a sequence of least squares problems. The solution of the least squares problem yields the estimated damping coefficients. The resulting experimentally determined analytical model is compared with the time histories via numerical simulation of the dynamic response. The suggested procedure is compared with a standard modal damping ratio model commonly used in experimental modal analysis.

Meirovitch, 2001 [11]. This book presents material fundamental to a modern treatment of vibrations. In this book, the focus is on analytical developments and computational solutions. A large number of examples and computer programs written in MATLAB are provided.

Boresi, 1985 [12]. This book presents an integration of both traditional methods and innovations in the field of engineering.

Clough and Penzien, 1993 [13]. In this book, the treatment of single-degree of freedom system, multi-degree of freedom discrete parameter systems and infinite degree of freedom continuous systems is presented.

Bhavikatti,1996 [14]. In this book all the basics of strength of materials are presented. Basic concepts on stress, strain, and theories of failure are elaborated.

III. MATHEMATICAL MODEL FORMULATION

3.0 INTRODUCTION:

In this chapter, a mathematical model of a cantilever beam under harmonic base excitation is developed. For this purpose, Euler Bernoulli beam theory has been applied. The dynamic response analysis of cantilever beam under base excitation is carried out using the modal superposition method.

3.1 Analytical Model of Cantilever Beam under Harmonic Base Excitation:

Figure 3.1 shows a cantilever beam close to that of a constant section Euler-Bernoulli beam under base excitation.

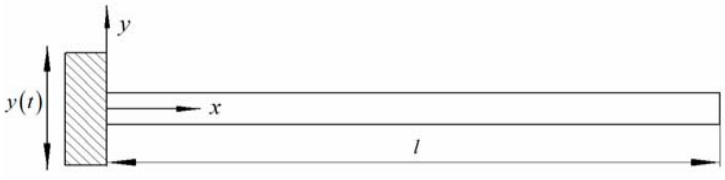

Fig. 3.1.Cantilever beam under base excitation [7]

Where, l= Length of the beam, E= Elastic Modulus, I= Moment of inertia,

m= mass of the beam per unit length, A= cross sectional area.

Figure 3.2 (a) shows a small segment of beam and in fig. 3.2(b) free body diagram of cross section is shown.

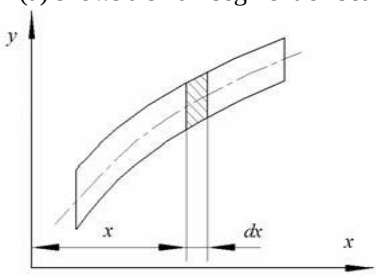

(a) A small segment of beam

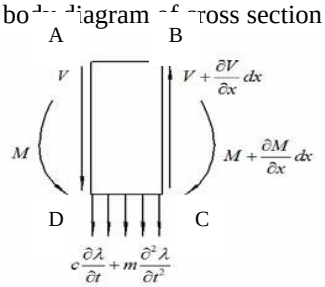

(b) Force analysis on the cross section

Fig.3.2.Force analysis [7]

In the fig. 3.2 (b), V=shear force on the vertical section, M= Bending Moment, C= velocity damping coefficient.

In this case, following sign convention is used

i. Force: upward positive, downward negative
ii. Moment: clockwise positive, anticlockwise negative

3.2 Dynamic Response Analysis: [7]

The total displacement of one point on the cantilever beam under base excitation is defined as,

$$\lambda(x,t) = y(t) + \varphi(x,t) \tag{3.1}$$

Where, $\varphi(x,t)$ =dynamic deflection curve, $y(t)$ = harmonic base excitation as $y(t) = Y\sin(\omega t)$

Where, ω = excitation frequency (rad/s), Y =displacement amplitude of the base excitation

A small segment is taken from the beam and the force analysis is carried out.

3.2.1 In this study two types of distributed viscous damping force are taken into consideration: [7]

1. External damping force $D(t)$,which is directly proportional to velocity $\frac{\partial \lambda}{\partial t}$

$$D(t) = -c\frac{\partial \lambda}{\partial t}$$

2. Internal damping force σ_r which is directly proportional to deformation velocity $\frac{\partial \varepsilon}{\partial t}$

$$\sigma_r = -c_r\frac{\partial \varepsilon}{\partial t}$$

Where, c_r = damping coefficient of deformation velocity, ε = strain.

Internal damping force can produce additional bending moment and shown in fig. 3.3

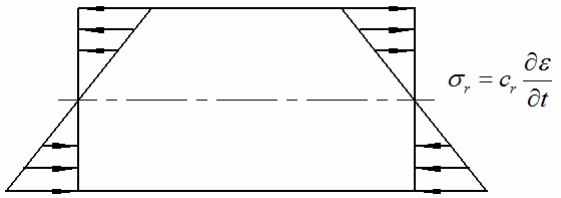

Fig.3.3.Bending moment produced from the internal damping force [7]

It is assumed that the strain distribution on the cross section is linear, and then the additional bending moment M_r produced by the internal damping force σ_r is given as,

$$M_r = \int_z \sigma_r z dA = \int_z c_r\frac{\partial \varepsilon}{\partial t} z dA \tag{3.2}$$

Where, z =distance between one point and the neutral axis

From the materials mechanics, the equation between strain and beam deflection is obtained as

$$\varepsilon = -z\frac{\partial^2(\varphi(x,t))}{\partial x^2} \tag{3.3}$$

3.2.2 Derivation of the equation (3.3): [12]

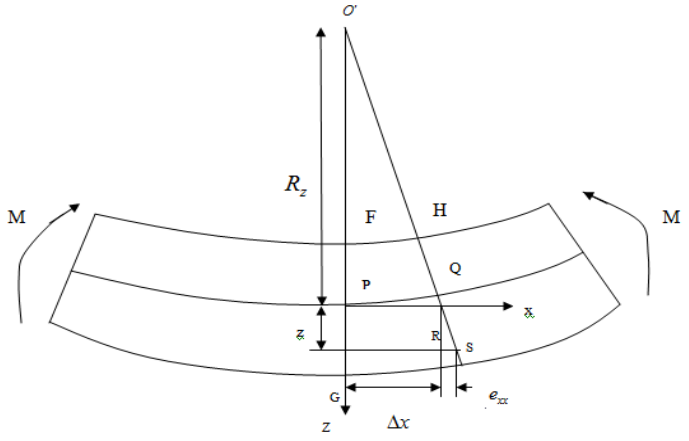

Fig.3.4.Deflected beam due to bending moment [12]

Here, variables and constants are taken as according to [7]. In the fig. 3.4,

O' = centre of the deflected beam and it lies on the negative side of z axis,

Δx = original length of cross section, e_{xx} = change in length of cross section,

R_z = distance of neutral axis from the O'.

We assume that deflections are small,

$$\frac{1}{R_z} \cong \frac{\partial^2(\varphi(x,t))}{\partial x^2} \tag{3.4}$$

$$\varepsilon_{xx} = \frac{e_{xx}}{\Delta x} \qquad e_{xx} = \varepsilon_{xx}(\Delta x)$$

□ O'PQ and □ QRS are similar triangles

$$\frac{-\Delta x}{R_z} = \frac{(\Delta x)\varepsilon_{xx}}{z}$$

Dividing both sides by (Δx) we obtain

$$-\frac{1}{R_z} = \frac{\varepsilon_{xx}}{z} \tag{3.5}$$

Now, from Eq. (3.4) and Eq. (3.5)

$$-\frac{\partial^2(\varphi(x,t))}{\partial x^2} = \frac{\varepsilon_{xx}}{z}$$

$$\varepsilon_{xx} = -z\frac{\partial^2(\varphi(x,t))}{\partial x^2}$$ Thus Eq. (3.3) is derived.

Substituting Eq. (3.3) into Eq. (3.2), the additional bending moment M_r becomes,

$$M_r = \int_z c_r \frac{\partial}{\partial t}\left[-z\frac{\partial^2(\varphi(x,t))}{\partial x^2}\right] zdA = -c_r \frac{\partial^3(\varphi(x,t))}{\partial x^2 \partial t}\int_z z^2 dA$$

$$= -c_r I \frac{\partial^3(\varphi(x,t))}{\partial x^2 \partial t} \tag{3.6}$$

$$I = \int_z z^2 dA$$

We have, $\frac{M_f}{I} = \frac{\sigma}{y} = \frac{E}{R}$ [14] from this, $M_f = \frac{EI}{R} = -EI\frac{\partial^2(\varphi(x,t))}{\partial x^2}$

Where, M_f =bending moment due to flexural formula

Then the total bending moment M of the small segment is,

$$M = -EI\frac{\partial^2(\varphi(x,t))}{\partial x^2} - c_r I\frac{\partial^3(\varphi(x,t))}{\partial x^2 \partial t} \tag{3.7}$$

From the moment balance of the whole small segment, let us take the moment about face BC in fig. 3.2(b).

$$M + \frac{\partial M}{\partial x}dx - M - Vdx + \frac{1}{2}\left[-c\frac{\partial(\lambda(x,t))}{\partial t} - m\frac{\partial^2(\lambda(x,t))}{\partial t^2}\right]dx^2 = 0 \tag{3.8}$$

Neglecting the high order item and referring to the Eq. (3.7), the Eq. (3.8) is simplified as,

$$V = \frac{\partial M}{\partial x} = \frac{\partial}{\partial x}\left[-EI\frac{\partial^2(\varphi(x,t))}{\partial x^2} - c_r I\frac{\partial^3(\varphi(x,t))}{\partial x^2 \partial t}\right] \tag{3.9}$$

Further, from the force balance of the whole small segment:

$$V + \frac{\partial V}{\partial x}dx - V - \left[m\frac{\partial^2(\lambda(x,t))}{\partial t^2} + c\frac{\partial(\lambda(x,t))}{\partial t}\right]dx = 0 \tag{3.10}$$

Substituting the expression of $\lambda(x,t)$ shown in eq. (3.1), the eq. (3.10) becomes,

$$\frac{\partial V}{\partial x}dx - \left[m\frac{\partial^2(y(t))}{\partial t^2} + m\frac{\partial^2(\varphi(x,t))}{\partial t^2} + c\frac{\partial(y(t))}{\partial t} + c\frac{\partial(\varphi(x,t))}{\partial x}\right]dx = 0 \tag{3.11}$$

Further simplification and organization implies,

$$\frac{\partial V}{\partial x} - m\frac{\partial^2(\varphi(x,t))}{\partial t^2} - c\frac{\partial(\varphi(x,t))}{\partial t} = m\frac{\partial^2(y(t))}{\partial t^2} + c\frac{\partial(y(t))}{\partial t} \tag{3.12}$$

At last, substituting the expression of V shown in Eq. (3.9) into the Eq. (3.12) gives the movement equation of the small segment under the sinusoidal base excitation and shown as,

$$EI\frac{\partial^4(\varphi(x,t))}{\partial x^4} + c_r I\frac{\partial^5(\varphi(x,t))}{\partial x^4\partial t} + m\frac{\partial^2(\varphi(x,t))}{\partial t^2} + c\frac{\partial(\varphi(x,t))}{\partial t} = -\left[m\frac{\partial^2(y(t))}{\partial t^2} + c\frac{\partial(y(t))}{\partial t}\right] \tag{3.13}$$

3.3 Dynamic Response of Cantilever Beam under Sinusoidal Base Excitation:

The vibration response $\lambda(t)$ of any point on the cantilever beam is $\lambda(t) = y(t) + \varphi(x,t)$, where, $\varphi(x,t)$ is the dynamic deflection curve of the beam. Here the modal superposition method is adopted to solve the expression of the dynamic deflection curve $\varphi(x,t)$. The every order natural frequency of the beam is set as ω_i, i =1, 2, 3… and the relative regular modal shape function is $Y_i(x)$, which satisfies orthogonalitly condition of as follows:

3.3.1 Orthogonalitly condition: [13]

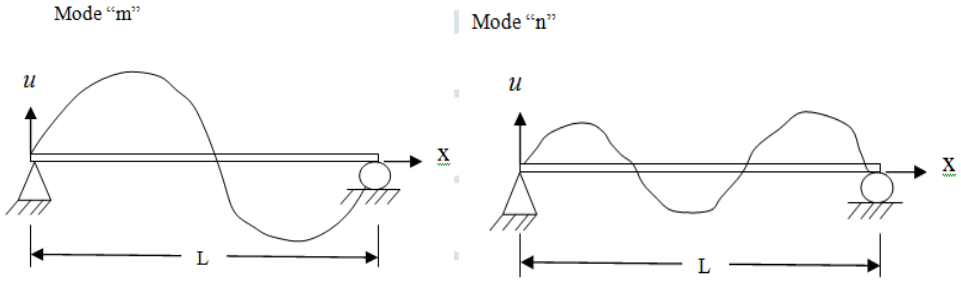

(a) Mode 'm' *(b) Mode 'n'*

Fig.3.5.Two modes of vibration for the same beam [13]

In the fig. 3.5,

Two different vibration modes 'm' (fig. 3.5(a)) and mode 'n' (fig. 3.5(b)) are shown for the same beam. In each mode displaced shape and inertial forces producing the displacements are indicated. In this case,

f_{I_m} =Inertial forces for mode 'm', f_{I_n} =Inertial forces for mode 'n',

$u_m(x,t)$ =displacement for mode 'm', $u_n(x,t)$ =displacement for mode 'n',

$Y_m(x)$ =shape function for mode 'm', $Y_n(x)$ =shape function for mode 'n',

$\eta_m(t)$ =Response function for mode 'm', $\eta_n(t)$ =Response function for mode 'n',

$m(x)$ =mass of beam= m.

If we apply Betties law to these two deflection patterns then, it states that "the work done by the inertial forces of mode 'n' acting on the deflection of mode 'm' is equal to the work of the inertial forces of mode 'm' acting on the displacement of mode 'n'". In other words,

$$\int_0^l u_m(x) f_{I_n}(x)dx = \int_0^l u_n(x) f_{I_m}(x)dx \tag{3.14}$$

$$u_m(x,t) = Y_m(x)\eta_m(t), \qquad u_n(x,t) = Y_n(x)\eta_n(t)$$

$$f_{I_m} = \omega_m{}^2 m Y_m(x)\eta_m(t), \qquad f_{I_n} = \omega_n{}^2 m Y_n(x)\eta_n(t)$$

Putting the values of displacements and inertia forces just defined into Eq. (3.14) we get,

$$(\omega_n{}^2 - \omega_m{}^2)\int_0^l Y_m(x)Y_n(x)m(x)dx = 0 \quad \text{Since } \omega_m \neq \omega_n \ (\omega_n{}^2 - \omega_m{}^2) \neq 0$$

Therefore, $\int_0^l Y_m(x)Y_n(x)m(x)dx = 0$ (3.15)

The normalizing procedure most often used in computer programs for structural vibration analysis, involves adjusting each modal amplitude to the amplitude Y_i which satisfies the condition,

$$Y_i^T m Y_i = 1$$

For scalar shape function $Y_i^T = Y_i$

Therefore orthogonalitly condition becomes,

$$\int_0^l m Y_i^2(x)dx = 1 \tag{3.16}$$

In the view of above condition the dynamic deflection curve $\varphi(x,t)$ is expressed by the regular response $\eta_i(t)$ and the regular modal shape $Y_i(x)$ using modal superposition method.

3.3.2 Modal superposition method: [13]

Any physically permissible displacement pattern can be made up by superposing appropriate amplitudes of the vibration mode shapes for the structure. The essential operation of the modal superposition analysis is the transformation from the geometric displacement coordinate to the modal amplitude or normal coordinates.

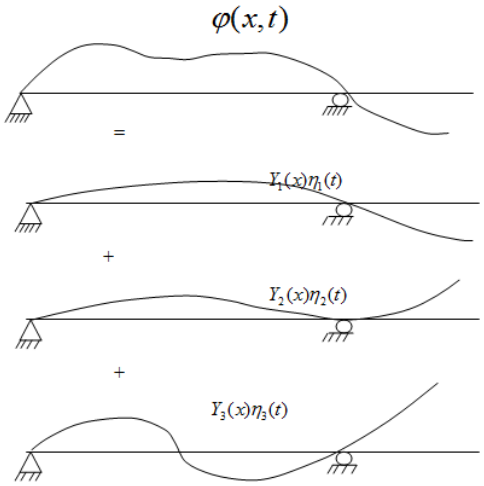

Figure 3.6 shows that, any arbitrary deflection of the beam is equal to the sum of various mode shapes of the same beam.

$$\varphi(x,t) = \sum_{i=1}^{\infty} Y_i(x)\eta_i(t) \tag{3.17}$$

Fig.3.6.Arbitrary beam displacements by normal coordinate [13]

3.3.3 Expression of $Y_i(x)$ for a cantilever beam: [11]

From a force balance and moment balance of a beam we get the following equation.

$$\frac{\partial^2}{\partial x^2}\left[EI\frac{\partial^2\varphi(x,t)}{\partial x^2}\right] + f(x,t) = m\frac{\partial^2\varphi(x,t)}{\partial t^2} \tag{3.18}$$

Where, *f(x,t)*=externally applied uniformly distributed dynamic load.

By separating shape function $\varphi(x,t)$ in the spatial variable x and t, and expressed as,

$$\varphi(x,t) = Y(x)\eta(t) \tag{3.19}$$

Putting Eq. (3.19) in the Eq. (3.18), $$\frac{d^2}{dx^2}\left[EI\frac{d^2Y(x)}{dx^2}\right] = -\omega^2 mY(x) \tag{3.20}$$

Hence the differential equation becomes, $$\frac{d^4Y(x)}{dx^4} + k^4Y(x) = 0 \tag{3.21}$$

Where, $$k^4 = \frac{\omega^2 m}{EI}$$

The boundary conditions for a cantilever beam are

$$Y(x) = 0 \quad \frac{dY(x)}{dx} = 0 \quad x = 0 \tag{3.22}$$

$$\frac{d^2Y(x)}{dx^2} = 0 \quad \frac{d^3Y(x)}{dx^3} = 0 \quad x = l \tag{3.23}$$

The general solution of Eq. (3.21) is

$$Y(x) = A\sin kx + B\cos kx + C\sinh kx + D\cosh kx \tag{3.24}$$

The first of boundary conditions (3.22) yields

$$Y(0) = B + D = 0 \qquad \text{So that,} \quad D = -B \tag{3.25}$$

For the second boundary condition we write

$$\frac{dY(x)}{dx} = k\left(A\cos kx - B\sin kx + C\cosh kx + D\sinh kx\right) \tag{3.26}$$

This yields, $\left.\frac{dY(x)}{dx}\right|_{x=0} = k(A + C) = 0 \qquad$ so that, $C = -A$ (3.27)

Hence, the solution reduces to

$$Y(x) = A(\sin kx - \sinh kx) + B(\cosh kx - \cos kx) \tag{3.28}$$

Before enforcing boundary conditions (3.23), we write

$$\frac{d^2Y(x)}{dx^2} = -k^2\left[A(\sin kx + \sinh kx) + B(\cos kx + \cosh kx)\right] \tag{3.29}$$

$$\frac{d^3Y(x)}{dx^3} = -k^3\left[A(\cos kx + \cosh kx) - B(\sin kx - \sinh kx)\right] \tag{3.30}$$

Using Eq. (3.29), the first of boundary conditions (3.23) yields

$$B = -\frac{\sin kl + \sinh kl}{\cos kl + \cosh kl}A \tag{3.31}$$

Inserting Eq. (3.31) into Eq. (3.30) and using second of boundary conditions (3.23), we obtain the characteristic equation

$$\cos kl + \cosh kl = -1 \tag{3.32}$$

Introducing Eq. (3.31) into Eq. (3.28), in conjunction with the eigen values $\beta_i L$, we write the eigen functions in the form

$$Y_i(x) = D_i\left[\sin k_i x - \sinh k_i x - \frac{\sin k_i l + \sinh k_i l}{\cos k_i l + \cosh k_i l}(\cos k_i x - \cosh k_i x)\right] \tag{3.33}$$

After rearranging the Eq. (3.33)

$$Y_i(x) = D_i\left[\cosh k_i x - \cos k_i x - \frac{\sinh k_i l - \sin k_i l}{\cosh k_i l + \cos k_i l}(\sinh k_i x - \sin k_i x)\right] \tag{3.34}$$

Where, D_i =Parameter related to the excitation level, k_i =Parameter related to natural frequency

Corresponding to the first five order, the values of k_i are as follows,

$\frac{1.875}{l}, \frac{4.694}{l}, \frac{7.855}{l}, \frac{10.996}{l}, \frac{14.137}{l}$ respectively.

Substituting Eq. (3.17) for $\varphi(x,t)$ into Eq. (3.13) for movement equation implies that,

$$EI\frac{\partial^4\left(\sum_{i=1}^{\infty}Y_i(x)\eta_i(t)\right)}{\partial x^4} + c_r I\frac{\partial^5\left(\sum_{i=1}^{\infty}Y_i(x)\eta_i(t)\right)}{\partial x^4\partial t} + m\frac{\partial^2\left(\sum_{i=1}^{\infty}Y_i(x)\eta_i(t)\right)}{\partial t^2} + c\frac{\partial\left(\sum_{i=1}^{\infty}Y_i(x)\eta_i(t)\right)}{\partial t} = -\left[m\frac{\partial^2(y(t))}{\partial t^2} + c\frac{\partial(y(t))}{\partial t}\right]$$

Simplifying further

$$\sum_{i=1}^{\infty}EI\frac{d^4\left(Y_i(x)\eta_i(t)\right)}{dx^4} + \sum_{i=1}^{\infty}c_r I\frac{d^4\left(Y_i(x)\dot{\eta}_i(t)\right)}{dx^4} + \sum_{i=1}^{\infty}mY_i(x)\ddot{\eta}(t) + \sum_{i=1}^{\infty}cY_i(x)\dot{\eta}_i(t) = -\left[m\frac{\partial^2(y(t))}{\partial t^2} + c\frac{\partial(y(t))}{\partial t}\right] \tag{3.35}$$

Utilizing the orthogonalitly conditions, the Eq. (3.35) is integrated along the longitudinal direction of the beam, which yields

$$\eta_i(t)\int_0^l EI\frac{d^4(Y_i(x))}{dx^4}Y_i(x)dx + \sum_{i=1}^{\infty}\dot{\eta}_i(t)\int_0^l\left[c_r I\frac{d^4(Y_i(x))}{dx^4} + cY_i(x)\right]Y_i(x)dx + \ddot{\eta}_i(t)\int_0^l mY_i^2(x)dx = F_i(t) \tag{3.36}$$

Where, $F_i(t) = \int_0^l -\left[m\frac{\partial^2(y(t))}{\partial t^2} + c\frac{\partial(y(t))}{\partial t}\right]Y_i(x)dx$

Assuming that the two damping coefficients c and c_r mentioned above are proportional respectively to mass m and modulus of elasticity E, we can write,

$c = \alpha m , c_r = \beta E$ where, α and β are constants.

The Eq. (3.36) is simplified as,

$$\ddot{\eta}_i(t) + \left(\alpha + \beta\omega_i^2\right)\dot{\eta}_i(t) + \omega_i^2\eta_i(t) = F_i(t) \tag{3.37}$$

Here, $\omega_i^2 = \int_0^l EI \frac{d^4(Y_i(x))}{dx^4} Y_i(x)dx$

Accordingly, $F_i(t) = \int_0^l -\left[m\frac{\partial^2(y(t))}{\partial t^2} + \alpha m \frac{\partial(y(t))}{\partial t} \right] Y_i(x)dx$

Furthermore, the i order modal damping ratio ζ_i is expressed as,

$$\zeta_i = \frac{\alpha + \beta\omega_i^2}{2\omega_i} = \frac{\alpha}{2\omega_i} + \frac{\beta\omega_i}{2} \tag{3.38}$$

$$\zeta_1 = \frac{\alpha}{2\omega_1} + \frac{\beta\omega_1}{2} \qquad \zeta_2 = \frac{\alpha}{2\omega_2} + \frac{\beta\omega_2}{2} \tag{3.39), (3.40}$$

After solving Eq. (3.39) and (3.40) for α and β the coefficients α , β are determined from the modal damping ratio and natural frequency, the solution formulas are,

$$\alpha = \frac{2\omega_1\omega_2\left(\zeta_1\omega_2 - \zeta_2\omega_1\right)}{\omega_2^2 - \omega_1^2} \qquad \beta = \frac{2\left(\zeta_2\omega_2 - \zeta_1\omega_1\right)}{\omega_2^2 - \omega_1^2} \tag{3.41), (3.42}$$

Where, ζ_1, ζ_2, ω_1, ω_2 can be obtained from the experiment. Combining Eq. (3.37) and Eq. (3.38) yields the final equation,

$$\ddot{\eta}_i(t) + 2\zeta_i\omega_i\dot{\eta}_i(t) + \omega_i^2\eta_i(t) = F_i(t) \tag{3.43}$$

The solution of Eq. (3.43) is easily obtained by reference to that of a single degree of freedom system and shown as,

$$\eta_i(t) = e^{(-\zeta_i\omega_i t)}\left[\frac{\dot{\eta}_{i0} + \zeta_i\omega_i\eta_{i0}}{\omega_i'} \sin\omega_i' t + \eta_{i0}\cos\omega_i' t + \frac{1}{\omega_i'}\int_0^t F_i(\tau)e^{(\zeta_i\omega_i\tau)}\sin\omega_i'(t-\tau)d\tau \right] \tag{3.44}$$

Where, $\omega_i' = \omega_i\sqrt{1-\zeta_i^2}$ [7] (3.45)

$$\eta_{i0} = \int_0^l m\varphi(x,0)Y_i(x)dx \qquad \dot{\eta}_{i0} = \int_0^l m\dot{\varphi}(x,0)Y_i(x)dx \tag{3.46), (3.47}$$

Finally the total displacement of the cantilever beam under sinusoidal base excitation is expressed as,

$$\lambda(x,t) = y(t) + \varphi(x,t) = y(t) + \sum_{i=1}^{\infty} Y_i(x)\eta_i(t) \tag{3.48}$$

From the Eq. (3.48) the dynamic response of cantilever beam under harmonic base excitation can be determined.

3.4 Solution Procedure to obtain the Dynamic Response Curve with the help of MATLAB Software:

In this section the solution of the Eq. (3.48) is obtained with the help of MATLAB software. This procedure is also explained step by step. The dynamic response curve obtained from the MATLAB software is presented. The specifications of cantilever beam subjected to base excitation are shown in section 3.4.1.

3.4.1 Cantilever beam specifications:

Beam type: Ti-6Al-4V

Physical and mechanical properties:

Density ρ =4500 kg/m3, Youngs modulus E=110GPa, Shear modulus G=45GPa, Bulk modulus K=150GPa,

Poissons ratio μ =0.35, Yield strength σ_y =900MPa

Ultimate strength= σ_u =950MPa, Mass per unit length=m=0.10125

Dimensions of the beam: Length L= 255mm, Width b= 15mm, Thickness t= 1.5mm

Note: 25mm section to be mounted in the clamping device. Therefore l= 230mm.

3.4.2 Solution procedure to obtain dynamic response curve:

Here dynamic response curve is obtained at x=0.150m from the fixed end of the cantilever beam. Amplitude of the base excitation Y is taken as 0.001m, base excitation frequency w is taken as 110 rad/s. Now, to plot the curve between independent variable t and the dependent variable $\lambda(x,t)$ below procedure is followed.

$$\lambda(x,t) = y(t) + \varphi(x,t) = y(t) + \sum_{i=1}^{\infty} Y_i(x)\eta_i(t)$$

In the equation, $y(t) = Y\sin(\omega t)$ the amplitude of base excitation is tentatively taken as Y=0.001m and the value of base excitation frequency w is taken near to the first natural frequency of the beam i.e. w=110 rad/s is also known,hence y (t) is the function of t only. MATLAB program is prepared for this equation.

Now, in the Eq. (3.34)

$$Y_i(x) = D_i\left[\cosh k_i x - \cos k_i x - \frac{\sinh k_i l - \sin k_i l}{\cosh k_i l + \cos k_i l}(\sinh k_i x - \sin k_i x)\right]$$

$D_i = \sqrt{\frac{1}{ml}}$ =6.55298 $k_1 l = 1.875$, $k_2 l = 4.694$, $k_3 l = 7.855$, $k_4 l = 10.996$, $k_5 l = 14.137$

,

$x = 0.150m$, $l = 0.230m$

MATLAB program for this equation is prepared and following values are obtained.

$Y_1(x) = 6.9201$, $Y_2(x) = 6.0844$, $Y_3(x) = -8.1536$, $Y_4(x) = 0.8125$, $Y_5(x) = 7.7983$.

Now, in the Eq.(3.44)

$$\eta_i(t) = e^{(-\zeta_i\omega_i t)}\left[\frac{\dot{\eta}_{i0} + \zeta_i\omega_i\eta_{i0}}{\omega_i'}\sin\omega_i' t + \eta_{i0}\cos\omega_i' t + \frac{1}{\omega_i'}\int_0^t F_i(\tau)e^{(\zeta_i\omega_i\tau)}\sin\omega_i'(t-\tau)d\tau\right]$$

The natural frequencies of the beam are calculated with the help of Euler Bernoulli equation as follows.

$\omega = k_n\sqrt{\frac{Et^2}{12\rho l^4}}$, k_n =3.52, 22.0, 61.7, 121, 200

$\omega_1 = 115.892\,rad/s$, $\omega_2 = 724.325\,rad/s$, $\omega_3 = 2031.4028\,rad/s$, $\omega_4 = 3983.788\,rad/s$, $\omega_5 = 6584.774\,rad/s$

ζ_i Is constant and it is obtained as follows

$$\zeta_i = \frac{\alpha + \beta\omega_i^2}{2\omega_i} = \frac{\alpha}{2\omega_i} + \frac{\beta\omega_i}{2} \qquad \alpha = 0.518,\ \beta = 3.168\times10^{-8}$$

Where,

$\zeta_1 = 0.002236$, $\zeta_2 = 3.69\times10^{-4}$, $\zeta_3 = 1.597\times10^{-4}$, $\zeta_4 = 1.28\times10^{-4}$, $\zeta_5 = 1.44\times10^{-4}$

Damped natural frequencies are calculated with the following equation.

$\omega_i' = \omega_i\sqrt{1-\zeta_i^2}$ Here, $\sqrt{1-\zeta_i^2} \approx 1$

Therefore, $\omega_1' = \omega_1$, $\omega_2' = \omega_2$, $\omega_3' = \omega_3$, $\omega_4' = \omega_4$, $\omega_5' = \omega_5$

$$\eta_{i0} = \int_0^l m\varphi(x,0)Y_i(x)dx \quad \varphi(x,0) = \sum_{i=1}^{\infty} Y_i(x)\eta_i(0) \quad \eta_i(0) = \left[\eta_{i0} - \frac{1}{\omega_i'}\int_0^t F_i(\tau)e^{(\zeta_i\omega_i\tau)}\sin\omega_i'(\tau)d\tau\right]$$

,

$$F_i(\tau) = \int_0^l -\left[m\frac{\partial^2(y(\tau))}{\partial\tau^2} + c\frac{\partial(y(\tau))}{\partial\tau}\right]Y_i(x)dx = lmY\omega Y_i(x)\left[\omega\sin(\omega\tau) - \alpha\cos(\omega\tau)\right]$$

Here MATLAB program is prepared to find the values of η_{i0}

$\eta_{10} = \eta_{20} = \eta_{30} = \eta_{40} = \eta_{50} = 0$

The same procedure is followed to find out the values of $\dot{\eta}_{i0}$, those values are as follows

$\dot{\eta}_{10} = \dot{\eta}_{20} = \dot{\eta}_{30} = \dot{\eta}_{40} = \dot{\eta}_{50} = 0$

Now, the MATLAB program is written for the Eq. (3.48) and the dynamic response curve is obtained as shown in the fig. (3.7(a)) and fig.(3.7(b))

Figure 3.7(a) shows the graph between dynamic deflection $\lambda(x,t)$ vs. time t between the time domains of 0s to 0.6s for the base excitation amplitude value Y=0.001m. Figure 3.7(b) shows the same graph for the base excitation amplitude value Y=0.0015m. Figure 3.7(c) shows the same graph for the base excitation amplitude value Y=0.002m

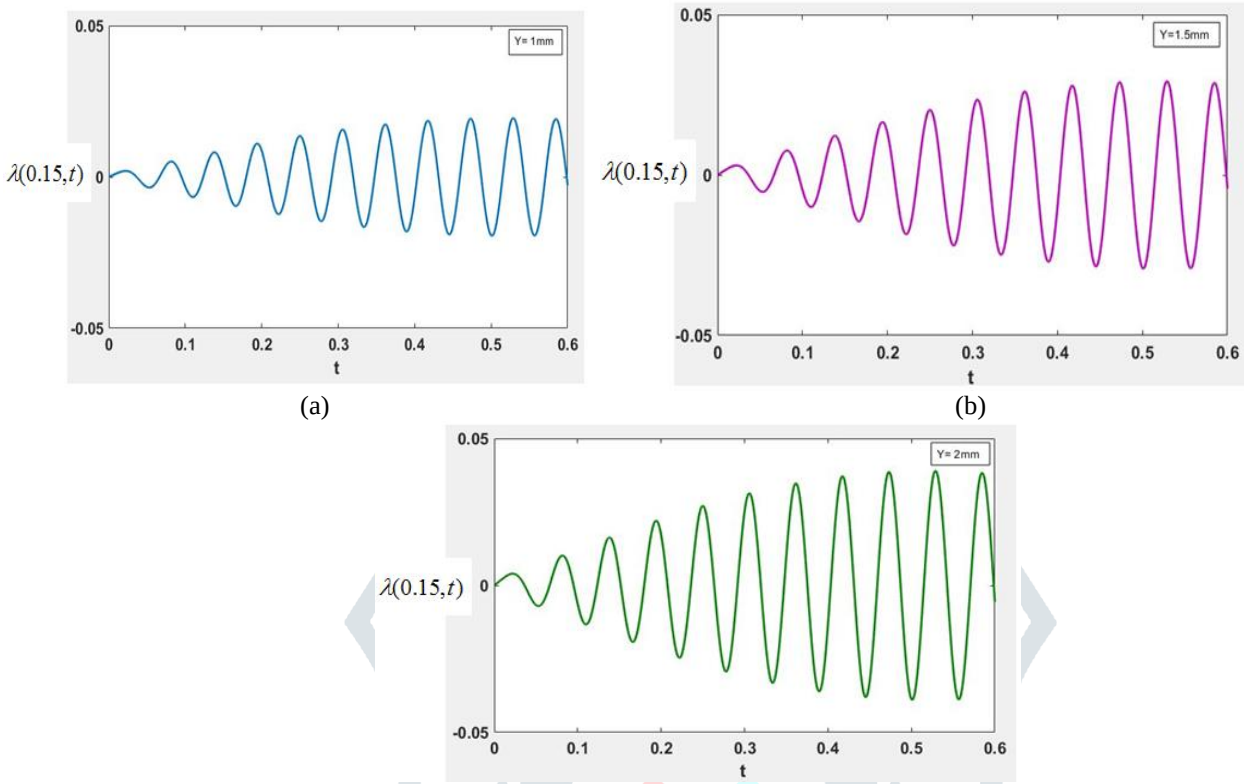

(a) (b)

(c)

Fig.3.7.Dynamic deflection $\lambda(0.15,t)$ (m) vs. time t(s), (a) Y=1mm, (b) Y=1.5mm, (c) Y=2mm

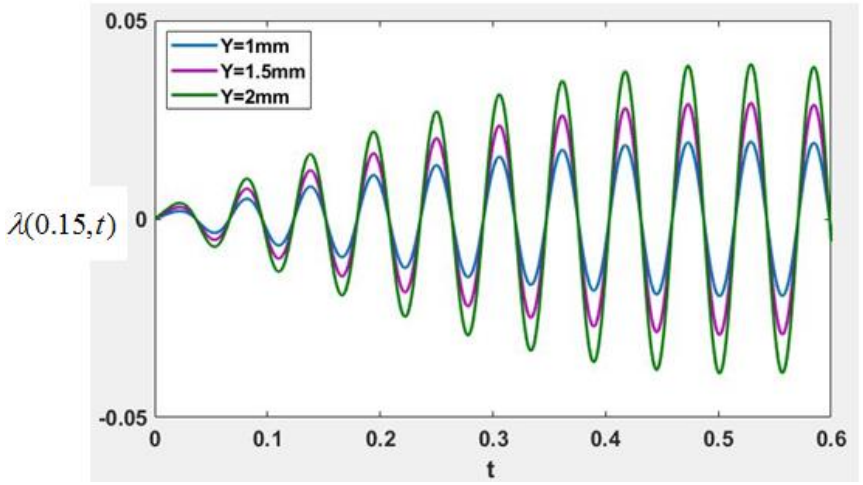

Fig.3.8.Dynamic deflection $\lambda(0.15,t)$ (m) vs. time t(s) combined

3.4.3 Solution procedure to obtain mode shapes of the cantilever beam:

In this case x is independent variable and is dependent variable. The value of t is taken as ten times the natural time period of the respective mode shape. Base excitation frequency is taken as the natural frequency w of the respective mode shape.

In order to obtain mode shapes the equation $\lambda(x,t) = y(t) + \varphi(x,t) = y(t) + \sum_{i=1}^{\infty} Y_i(x)\eta_i(t)$ can be written for different mode shapes separately as follows and separate MATLAB program is prepared for each mode shape.

For first mode shape $\lambda(x,t) = Y_1(x)\eta_1(t)$, for second mode shape $\lambda(x,t) = Y_2(x)\eta_2(t)$

For third mode shape $\lambda(x,t) = Y_3(x)\eta_3(t)$, for fourth mode shape $\lambda(x,t) = Y_4(x)\eta_4(t)$

For fifth mode shape $\lambda(x,t) = Y_5(x)\eta_5(t)$

Figure 3.8 (a), (b), (c), (d) and (e) are the first, second, third, fourth and fifth mode shapes respectively.

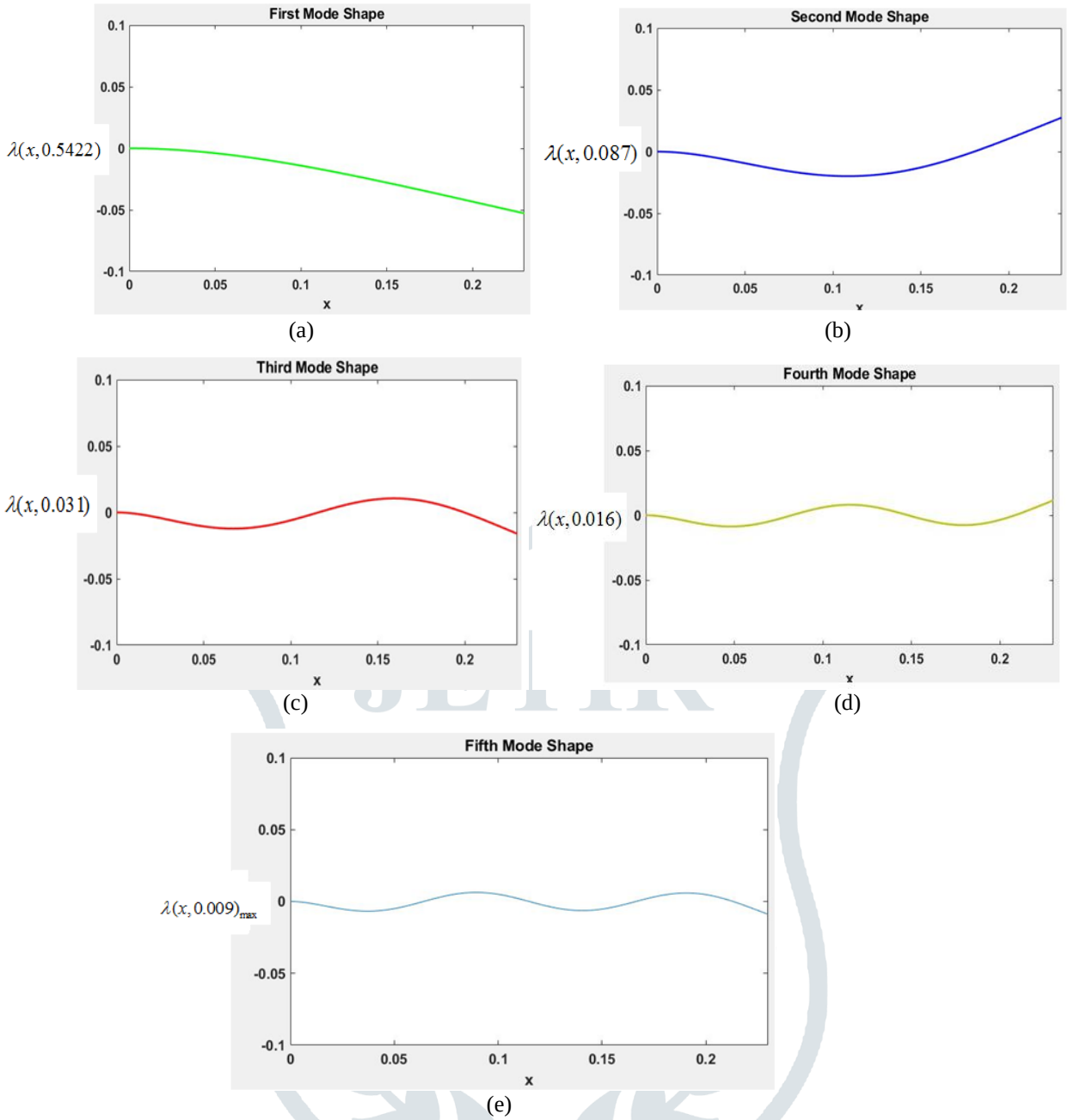

Fig.3.8. Dynamic deflection $\lambda(x,t)$ (m) vs. Location from the clamped end x (m)

Figure 3.9 shows combined mode shapes in a single graph.

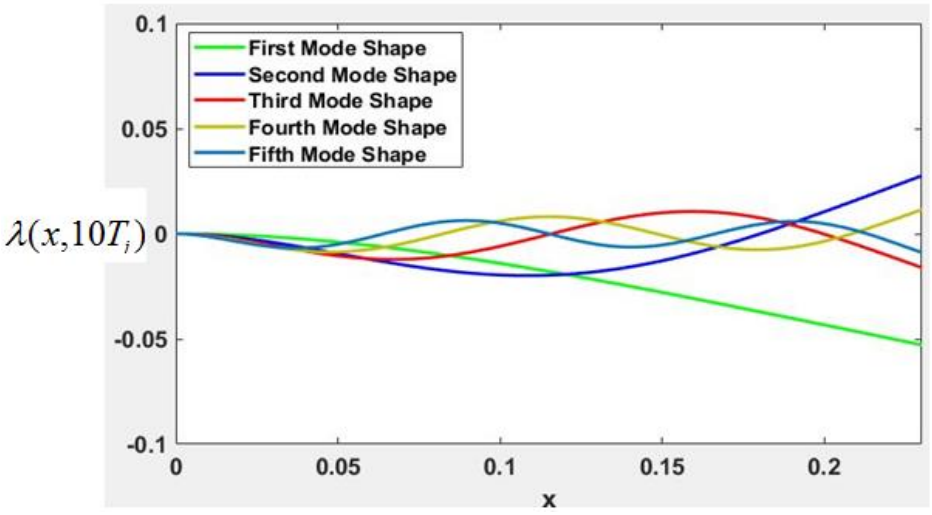

Fig.3.9. Dynamic deflection $\lambda(x,t)$ (m) vs. Location from the clamped end x (m)

Figure 3.10show that, as we go to the higher modes, the value of first maximum amplitude goes on decreasing. Also the x location from the clamped end where the first maximum amplitude is obtained goes on decreasing with increasing modes.
Similarly, Fig.3.11 shows that, Maximum beam deflection value goes on decreasing exponentially with increasing mode shapes.

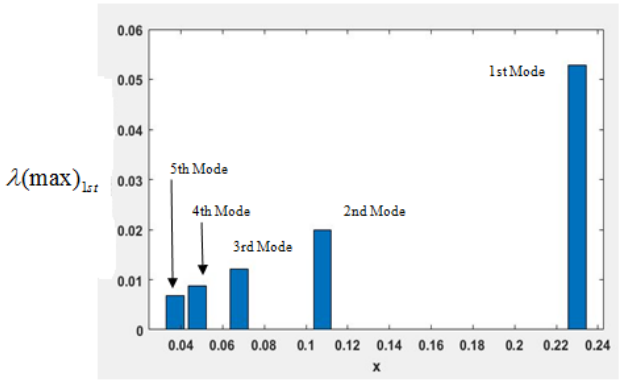

Fig.3.10. First max amplitude $\lambda(\max)_{1st}$ *(m) vs. x(m)*

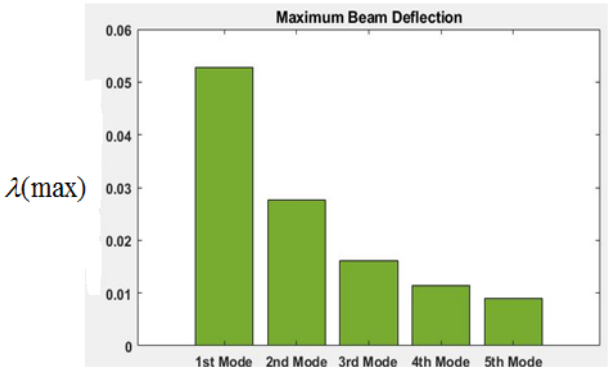

Fig.3.11.Maximum beam deflection $\lambda(\max)$ *(m) vs. no. of modes*

3.4.4 Effect of external damping c and internal damping c_r *on the dynamic response*

1. Constant internal damping c_r =3484.8, varying external damping c

Figure 3.12 shows the graph between maximum dynamic deflections at x location of 0.15m vs. external damping c at constant internal damping c_r . It indicates that, as external damping c value increases maximum dynamic deflection value decreases. It decreases with very high rate up to the c =1 but after that it decreases with very less rate.

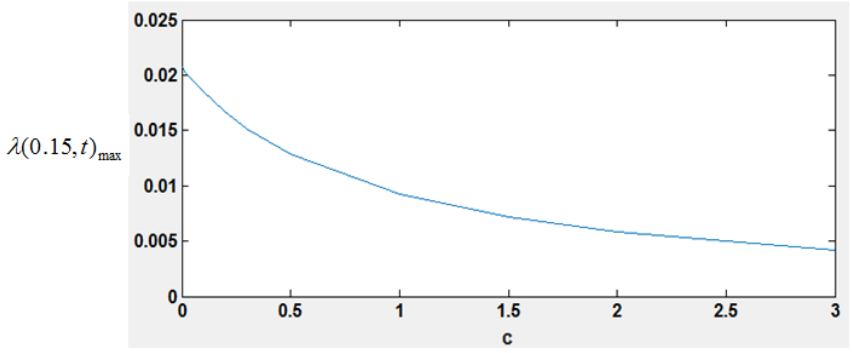

Fig.3.12.Maximum dynamic deflection $\lambda(0.15,t)_{\max}$ *(m) vs. external damping c*

2. Constant external damping c, varying internal damping c_r

Figure 3.13 shows that maximum dynamic deflection $\lambda(0.15,t)_{\max}$ does not change considerably with respect to the change in internal damping c_r value.

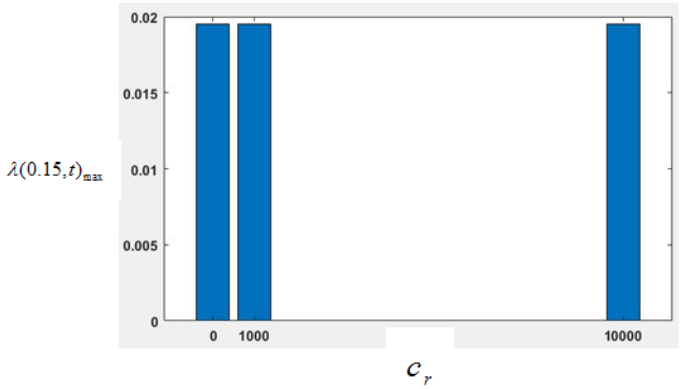

Fig.3.13.Maximum dynamic deflection $\lambda(0.15,t)_{\max}$ *(m) vs. internal damping* c_r

3. Dynamic response curve by taking internal damping c_r =0

Below figures show dynamic deflection at x location of 0.15m from the clamped end $\lambda(0.15,t)$ vs. time t by taking internal damping c_r =0. Figures 3.14(a), (b) and (c) are drawn at base excitation amplitudes of 1mm, 1.5mm and 2mm respectively. Figure 3.14(d) is combined graphs of fig. 3.14 (a), (b) and (c). From this analysis it is observed that, dynamic deflection curves obtained without considering internal damping c_r is exactly coinciding with the dynamic deflection curves obtained by considering internal damping c_r . Hence it can be concluded that internal damping c_r does not take much role in the dynamic deflection of the beam.

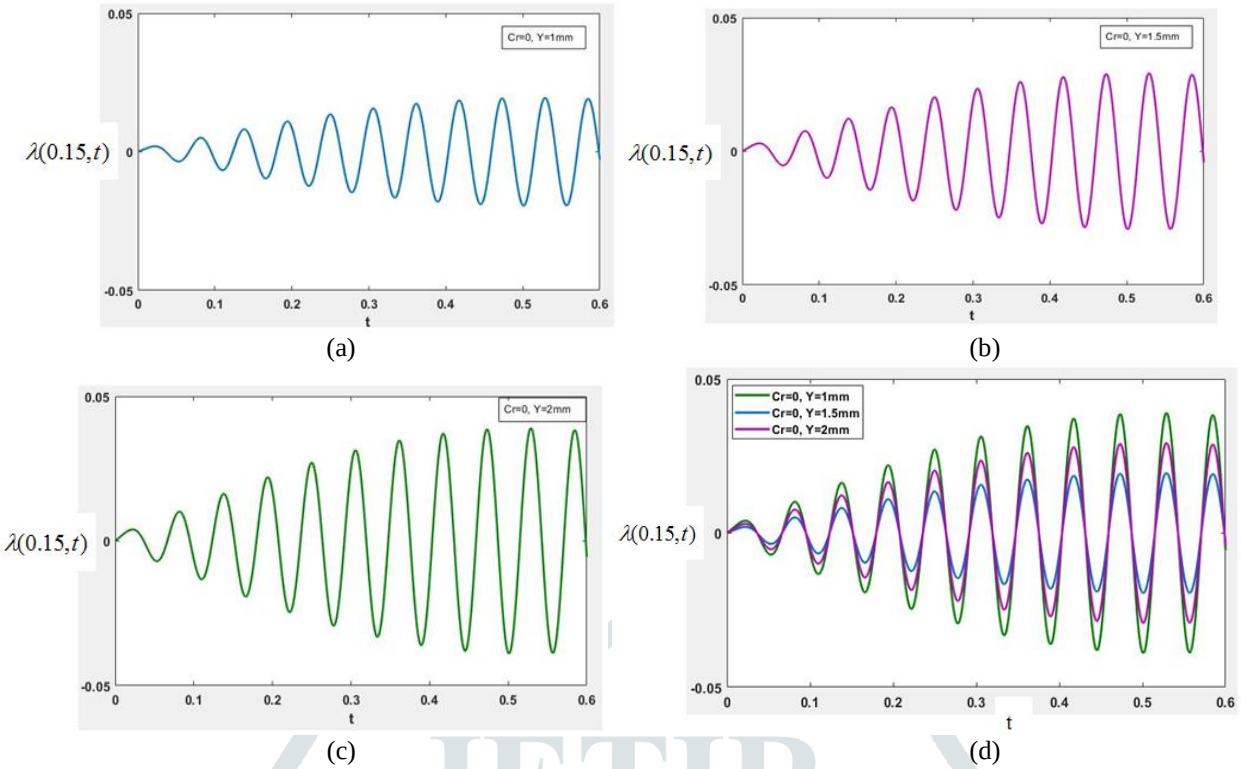

Fig.3.14.Dynamic deflection $\lambda(0.15,t)$ (m) vs. time t(s)

3.4.5 Dynamic response analysis of the same cantilever beam by considering base as fixed and applying external excitation force at x location of 0.15m from the fixed end.

Figure 3.15 shows the same cantilever beam fixed at one end and externally applied dynamic load $f(x,t)$ at location x=0.15m.

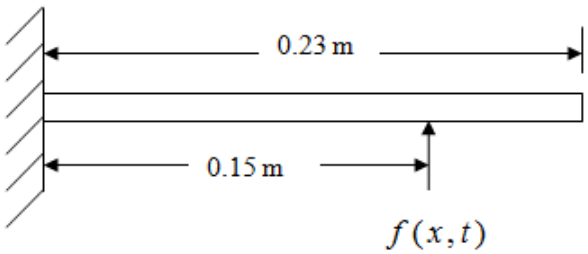

Fig.3.15.Cantilever beam with fixed base and applied dynamic load $f(x,t)$ at x location 0.15m

Governing differential equation of the beam

$$EI\frac{\partial^4(\psi(x,t))}{\partial x^4}+m\frac{\partial^2(\psi(x,t))}{\partial t^2}=f(x,t)$$

$\psi(x,t)$ =dynamic deflection of the beam

Where,

Boundary Conditions

1 Free end:

Bending moment = $EI\frac{\partial^2(\psi(x,t))}{\partial x^2}=0$

2 Fix end:

Deflection = $\psi(x,t)$ =0, slope= $\frac{\partial\psi(x,t)}{\partial x}=0$

In this case $\psi(x,t)$ becomes the total dynamic deflection and its equation is,

$$\psi(x,t)=\sum_{i=1}^{\infty}Y_i(x)\eta_i(t)$$

Where, $Y_i(x)$ is the mode shape equation of the beam and it is as shown below

$$Y_i(x) = D_i\left[\cosh k_i x - \cos k_i x - \frac{\sinh k_i l - \sin k_i l}{\cosh k_i l + \cos k_i l}(\sinh k_i x - \sin k_i x)\right]$$

$\eta_i(t)$ Is the time function equation of the beam and it is as shown below

$$\eta_i(t) = A_i \cos(\omega_i t) + B_i \sin(\omega_i t) + \frac{1}{mb\omega_i}\int_0^t F_i(\tau)\sin(\omega_i(t-\tau))d\tau$$

Where, $F_i(\tau) = \int_0^l f(x,t)Y_i(x)dx$, $b = \int_0^l Y_i(x)^2 dx$, $f(x,t) = F_0 \sin(\omega t)$

Here, MATLAB program is prepared for the total dynamic deflection equation $\psi(x,t)$ and following two graphs have been plotted.

1 Graph between dynamic deflection $\psi(0.15,t)$ (m) vs. time t (s) at various initial excitation force F_0 and at constant force excitation frequency $\omega = 110$ rad/s, as shown in fig.3.16.

Figure3.16 shows that dynamic deflection $\psi(0.15,t)$ increases with the increase in the initial excitation force F_0.

2 Graph between maximum dynamic deflection $\psi(x,t)_{max}$ (m) vs. force excitation frequency ω (rad/s) at constant excitation force F_0 =1N, as shown in fig.3.17.

Figure 3.17 shows that as there is increase in the force excitation frequency ω from 90 rad/s to first natural frequency of the cantilever beam that is 115.8 rad/s, the maximum dynamic deflection value $\psi(0.15,t)_{max}$ increases continuously. After that it decreases continuously with the further increase in the ω value.

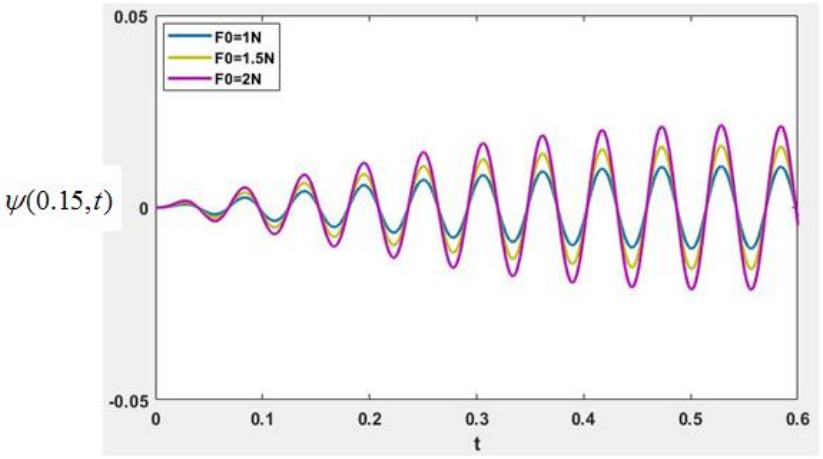

Fig.3.16.Dynamic deflection $\psi(0.15,t)$ (m) vs. time t (s)

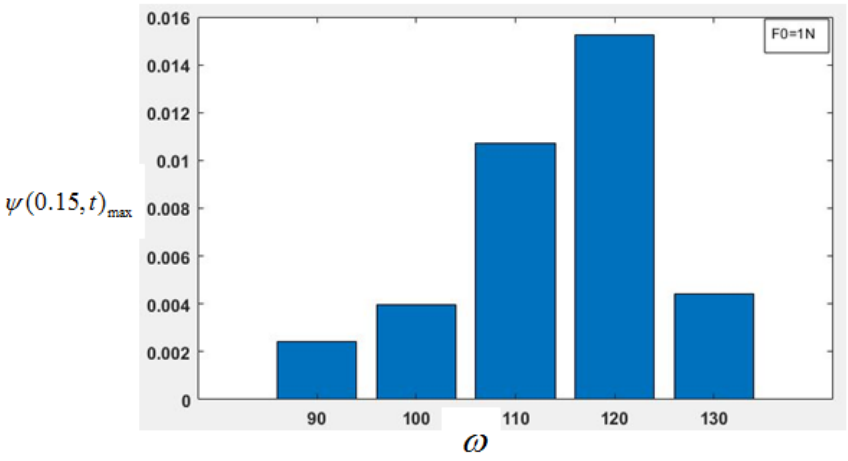

Fig.3.17.Maximum dynamic deflection $\psi(0.15,t)_{max}$ (m) vs. force excitation frequency ω (rad/s)

Closure: In this chapter mathematical model of the cantilever beam subjected to base excitation has been prepared. Then the governing differential equation of this system and its solution is obtained. MATLAB program is prepared to obtain dynamic response curves and mode shapes of the beam. The effect of internal damping c and external damping c_r on the dynamic response is shown. Then in the end mathematical model for the equivalent cantilever beam system but fixed at one end and applied external

excitation force at 0.15m from the fixed end is prepared. Governing differential equation and its solution is obtained. Again MATLAB program is prepared to obtain the dynamic response for this system.

IV. DYNAMIC RESPONSE ANALYSIS BY VARYING DIMENSIONS AND MATERIAL

4.0 INTRODUCTION:

In this chapter, the effect of variation of dimensions as well as the effect of variation of material on the dynamic response of the cantilever beam has been shown. In section 4.1 dimensions are varied by varying width b to thickness t ratio for the same material of previous chapters i.e. Ti-6Al-4V. In section 4.2 AISI 1065 material has been taken and dimensions are kept as same as in the previous chapters i.e. length l=230mm, width b=15mm, thickness t=1.5mm.

4.1 Dynamic Response Analysis by Varying Dimensions (Width b to Thickness t Ratio):

In this section dynamic response curves are obtained for three different values of b by t ratio and for each value of b by t ratio four different values of b and t are taken as shown in the table 4.1. Hence twelve different dynamic response curves are obtained. As there is variation in the dimension there is variation of certain values in the MATLAB program of dynamic response.

Table4.1. Values of b and t for different b/t ratio

b/t	b (mm)				t (mm)			
5	2.5	5	7.5	10	0.5	1	1.5	2
10	5	10	15	20	0.5	1	1.5	2
15	7.5	15	22.5	30	0.5	1	1.5	2

The following constant or variable values vary for respective value of width b and thickness t.

Mass per unit length m varies, hence constant term D_i varies since $D_i = \sqrt{\frac{1}{ml}}$

Thickness t varies hence natural frequency ω_i varies since $\omega = k_n \sqrt{\frac{Et^2}{12\rho l^4}}$

As there is variation in natural frequency ω_i, ζ_i varies since $\zeta_i = \frac{\alpha}{2\omega_i}$

Note: From the section 3.4.4 it has been concluded that internal damping is not taking much role in the dynamic response; hence internal damping c_r is taken as zero.

Note: Here external damping coefficient c is assumed as constant for all the variations and it is taken as 0.05245.

In the equation $c = \alpha m$ as c is constant and m is varying α varies with respect to m.

The changed values for respective width b to thickness t have shown in the following respective table.

4.1.1 Dynamic response curves for b/t=5:

The following parameter values of the table replaced in the dynamic response program and respective response curve is obtained.

Table4.2. Parameters for b/t=5

b, t	M	D_i	ω_1	ω_2	ω_3	ω_4	ω_5	α	ζ_1	ζ_2	ζ_3	ζ_4	ζ_5
2.5,0.5	0.0056	27.86	38.63	241.44	677.13	1327.9	2194.9	9.36	0.121	0.019	0.0069	0.0035	0.0021
5,1	0.0225	13.9	77.26	482.9	1354.3	2655.9	4390	2.33	0.015	0.0024	0.0008	0.0004	0.0002
7.5,1.5	0.051	9.23	115.89	724.35	2031.5	3983.9	6585	1.03	0.0044	0.0007	0.0002	0.0001	0.00007
10,2	0.09	6.95	154.53	965.8	2708.6	5311.9	8780	0.58	0.002	0.0003	0.0001	0.00005	0.00003

Figure 4.1 shows dynamic response curves for width b to thickness t ratio equal to 5 obtained at different values of width b and thickness t such that. Figure 4.1(a) is obtained at width b=2.5mm and thickness t=0.5mm and at base excitation frequency ω =30rad/s. Figure 4.1(b) is obtained at b=5mm and t=1mm and at ω =70rad/s. Figure 4.1(c) is obtained at b=7.5mm and t=1.5mm and at ω =110rad/s. Figure 4.1(d) is obtained at b=10mm and t=2mm and at ω =150rad/s

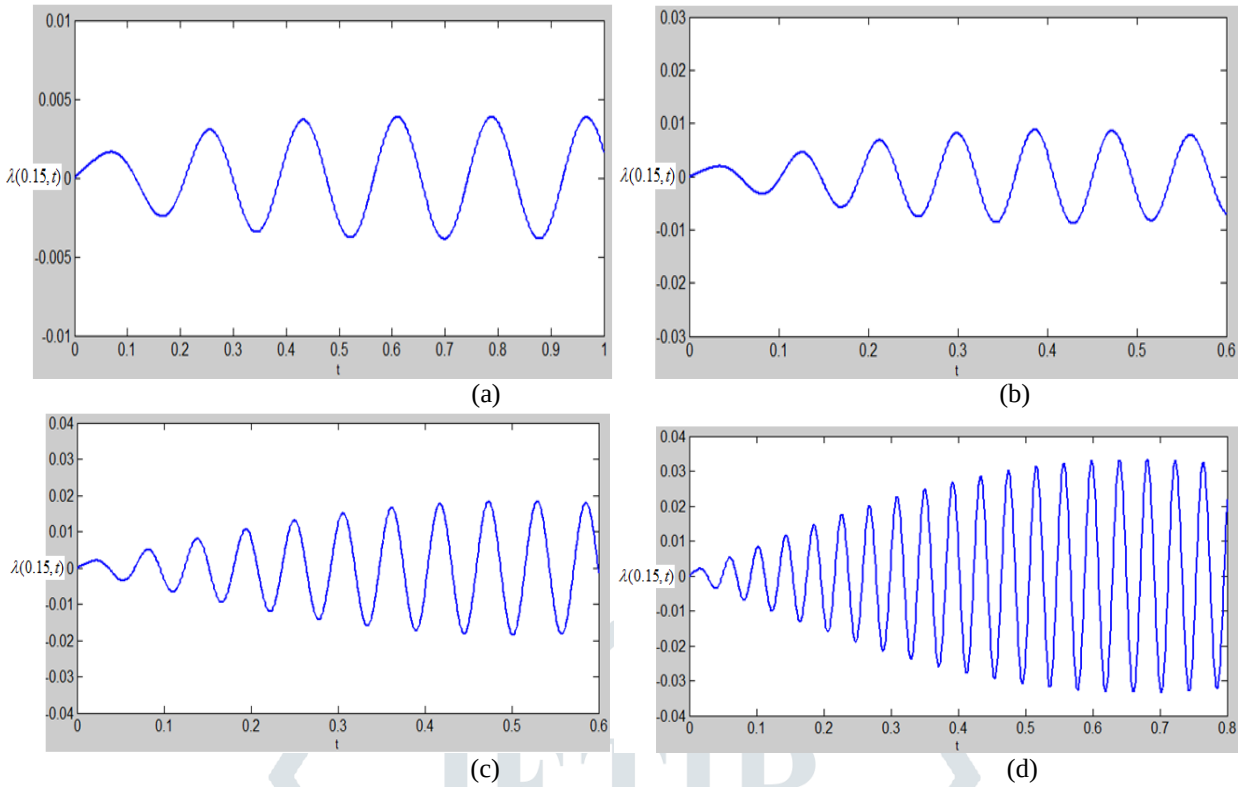

Fig.4.1. Dynamic deflection $\lambda(0.15,t)$ (m) vs. time t(s) for b/t=5

Figure 4.2 shows Maximum dynamic deflection $\lambda(0.15,t)_{\max}$ obtained from the fig.4.1 (a), (b), (c) and (d) respectively.

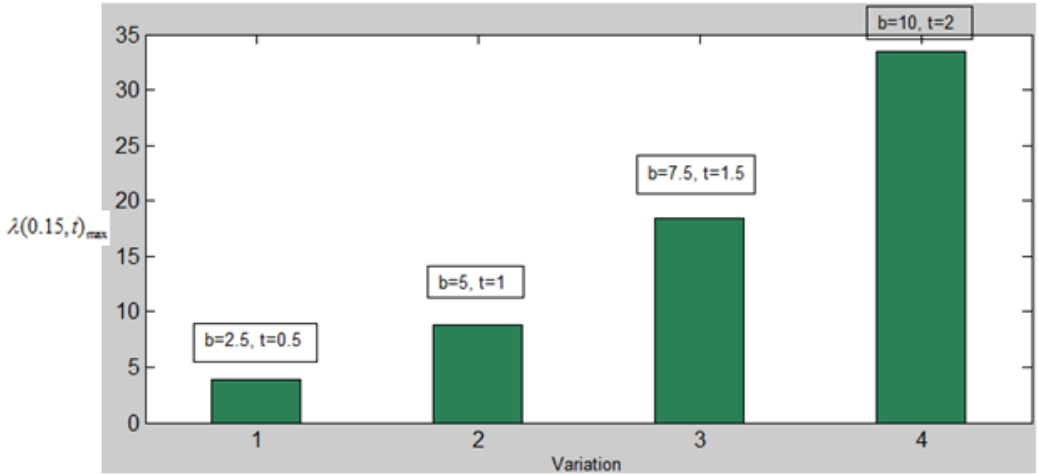

Fig.4.2.Maximum dynamic deflection $\lambda(0.15,t)_{\max}$ (mm) vs. Variations for b/t=5

4.1.2 Dynamic response curves for b/t=10:

The following parameter values of the table replaced in the dynamic response program and respective response curve is obtained.

Table4.3. Parameters for b/t=10

b, t	M	D_i	ω_1	ω_2	ω_3	ω_4	ω_5	α	ζ_1	ζ_2	ζ_3	ζ_4	ζ_5
5,0.5	0.01125	18.68	38.63	241.44	677.13	1327.9	2194.9	4.66	0.06	0.0096	0.0034	0.0017	0.0011
10,1	0.045	9.335	77.26	482.9	1354.3	2655.9	4390	1.16	0.0075	0.0012	0.00043	0.00022	0.00013
15,1.5	0.10125	6.22	115.89	724.35	2031.5	3983.9	6585	0.52	0.0022	0.00036	0.00013	0.000065	0.00004
20,2	0.18	4.668	154.53	965.8	2708.6	5311.9	8780	0.29	0.00094	0.00015	0.00005	0.000027	0.000002

Figure 4.3 shows dynamic response curves for width b to thickness t ratio equal to 10 obtained at different values of width b and thickness t such that. Figure 4.3(a) is obtained at width b=5mm and thickness t=0.5mm and at base excitation frequency ω =30rad/s. Figure 4.3(b) is obtained at b=10mm and t=1mm and at ω =70rad/s. Figure 4.3(c) is obtained at b=15mm and t=1.5mm and at ω =110rad/s. Figure 4.3(d) is obtained at b=20mm and t=2mm and at ω =150rad/s

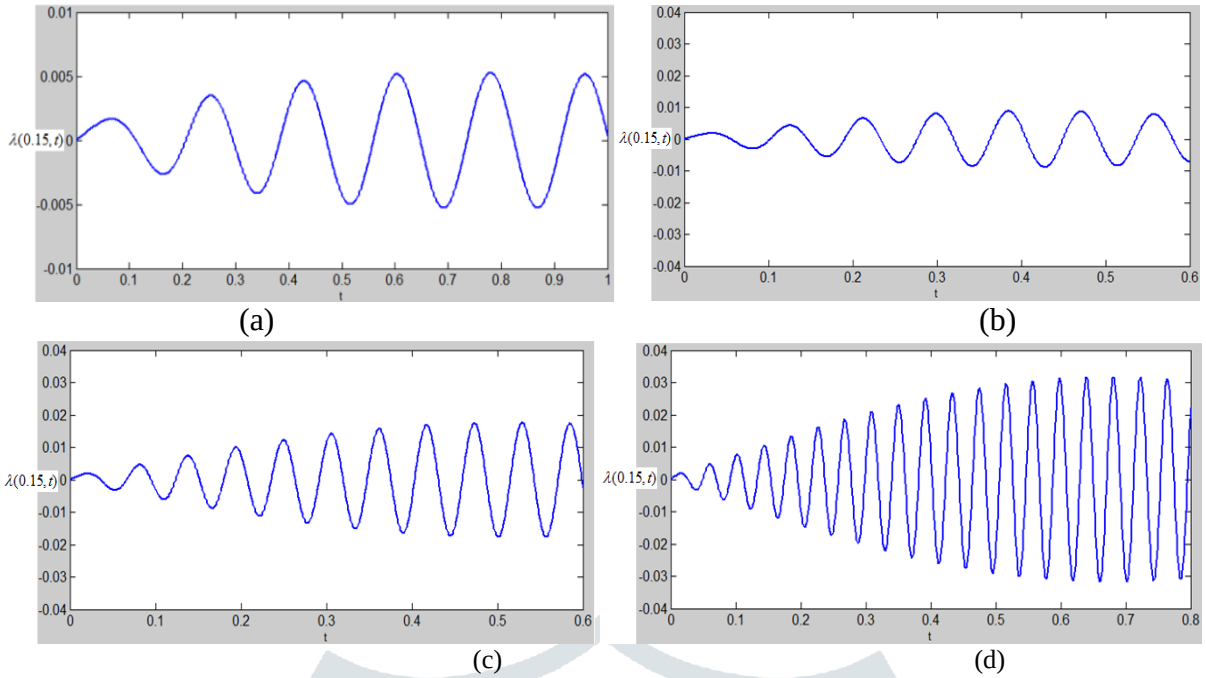

Fig.4.3. Dynamic deflection $\lambda(0.15,t)$ (m) vs. time t(s) for b/t=10

Figure 4.4 shows Maximum dynamic deflection $\lambda(0.15,t)_{max}$ obtained from the fig.4.3 (a), (b), (c) and (d) respectively.

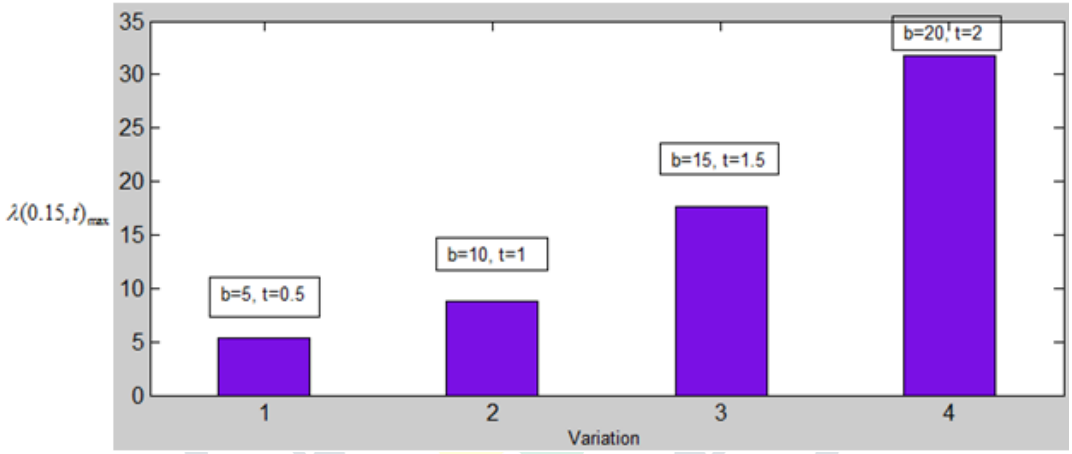

Fig.4.4. Maximum dynamic deflection $\lambda(0.15,t)_{max}$ (mm) vs. Variations for b/t=10

4.1.3 Dynamic response curves for b/t=15:

The following parameter values of the table replaced in the dynamic response program and respective response curve is obtained.

Table4.4. Parameters for b/t=15

b, t	M	D_i	ω_1	ω_2	ω_3	ω_4	ω_5	α	ζ_1	ζ_2	ζ_3	ζ_4	ζ_5
7.5,0.5	0.017	15.2	38.63	241.44	677.13	1327.9	2194.9	3.08	0.04	0.0064	0.0023	0.0012	0.0007
15,1	0.067	7.56	77.26	482.9	1354.3	2655.9	4390	0.78	0.005	0.0008	0.0003	0.00015	0.00009
22.5,1.5	0.152	5.08	115.89	724.35	2031.5	3983.9	6585	0.34	0.0015	0.0002	0.00008	0.000043	0.000026
30,2	0.27	3.81	154.53	965.8	2708.6	5311.9	8780	0.19	0.0006	0.0001	0.00004	0.000018	0.000011

Figure 4.5 shows dynamic response curves for width b to thickness t ratio equal to 15 obtained at different values of width b and thickness t such that. Figure 4.5(a) is obtained at width b=7.5mm and thickness t=0.5mm and at base excitation frequency ω =30rad/s. Figure 4.5(b) is obtained at b=15mm and t=1mm and at ω =70rad/s. Figure 4.5(c) is obtained at b=22.5mm and t=1.5mm and at ω =110rad/s. Figure 4.5(d) is obtained at b=30mm and t=2mm and at ω =150rad/s.

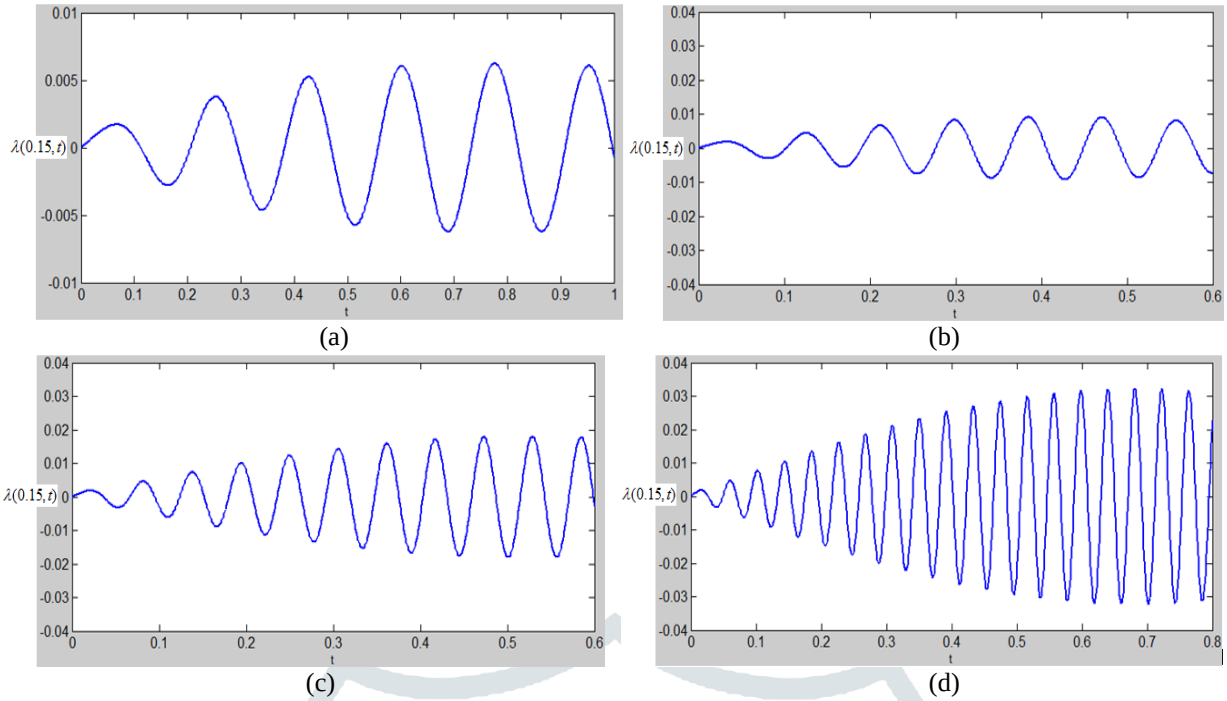

Fig.4.5. Dynamic deflection $\lambda(0.15,t)$ (m) vs. time t(s) for b/t=15

Figure 4.6 shows Maximum dynamic deflection $\lambda(0.15,t)_{\max}$ obtained from the fig.4.5 (a), (b), (c) and (d) respectively.

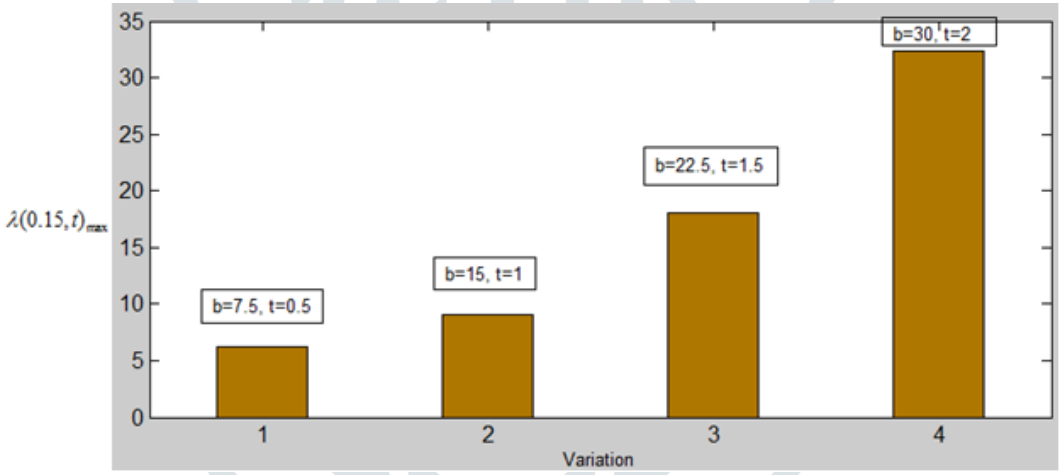

Fig.4.6. Maximum dynamic deflection $\lambda(0.15,t)_{\max}$ (mm) vs. Variations for b/t=15

4.2 Dynamic Response Analysis by Changing Material (AISI 1065):

In this section dynamic response curve is obtained for AISI 1065 material.

4.2.1 Cantilever beam specifications:

Beam type: AISI 1065

Physical and mechanical properties:

Density ρ =7850kg/m3, Youngs modulus E=200GPa, Shear modulus G=80GPa, Bulk modulus K=140GPa,

Poissons ratio μ =0.27, Yield strength σ_y =490MPa, Ultimate strength= σ_u =635MPa, Mass per unit length=m=0.1766

Dimensions of the beam: Length L= 255mm, Width b= 15mm, Thickness t= 1.5mm

Note: 25mm section to be mounted in the clamping device. Therefore= 230mm.

4.2.2 Solution Procedure:

Mass per unit length $m = \dfrac{M}{l}$ where, M= Total mass of the beam = $\rho V = \rho lbt$

Therefore $m = \rho bt$ =0.1766, $D_i = \sqrt{\dfrac{1}{ml}} = 4.96$, $\omega_i = k_n \sqrt{\dfrac{Et^2}{12\rho l^4}}$

ω_1 =145.435 rad/s, ω_2 =908.965 rad/s, ω_3 =2549.234 rad/s, ω_4 =5000 rad/s, ω_5 =8263.32 rad/s

Note: Internal damping is neglected and external damping coefficient is taken as 0.05245.

$c = \alpha m$, α =0.2969, $\zeta_i = \dfrac{\alpha}{2\omega_i}$

ζ_1 =0.00102, ζ_2 =0.0001633, ζ_3 =0.000058, ζ_4 =0.000029, ζ_5 =0.00001796

Figure 4.7 shows Dynamic deflection $\lambda(0.15,t)$ (m) vs. time t(s) for AISI 1065 material obtained by putting all the above values of parameters and constants in the MATLAB program.

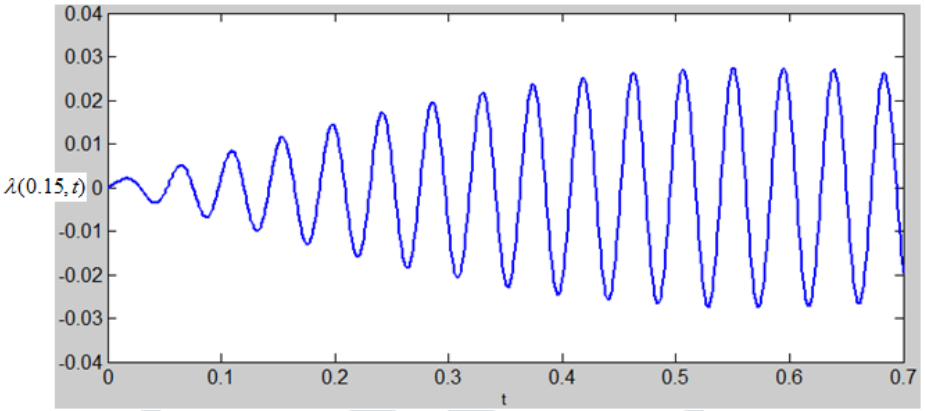

Fig.4.7. Dynamic deflection $\lambda(0.15,t)$ (m) vs. time t(s) for AISI 1065

Closure: In this chapter, the effect of variation of dimensions as well as the effect of variation of material on the dynamic response of the cantilever beam has been shown. Three different values of b/t ratio i.e. 5, 10 and 15 are taken and for each value of b/t ratio four different values of b and t are taken. Corresponding changes in the values of constants and variables which are dependent on the values of b and t have been made and MATLAB program is prepared accordingly. Hence twelve different response curves have been plotted and analyzed. Also the dynamic response curve for AISI 1065 material has been plotted by keeping the dimensions of the beam as in the previous chapter.

V. CONCLUSIONS

1. For base excitation amplitude values of 1mm, 1.5mm and 2mm respective maximum dynamic deflection values at x location of 150mm from the clamped location are 19.51mm, 29.26mm, 39.01mm. Hence it can be concluded that as base excitation amplitude Y increases, the maximum dynamic deflection at particular x location also increases.
2. From the obtained mode shapes of the cantilever beam, it is concluded that, at node points (where there is no deflection), designer can attach accessories which requires zero deflection. Also at maximum deflection point, the designer can attach damper to reduce deflection of the beam.
3. For constant external damping c =0.05245, if internal damping c_r is increased from 0 to 10000, maximum dynamic deflection is remaining constant for all the internal damping coefficient c_r values. Hence it is concluded that, the effect of internal damping c_r is very minute in the dynamic response of the beam and hence designer may not be taken into consideration while designing the cantilever beam type structures.
4. As external damping coefficient c increases from 0 to 3, maximum dynamic deflection λ_{max} value decreases from 20.75mm to 4.19mm. From c =0 to 1.5 λ_{max} is decreasing rapidly i.e. 20.75mm to 7.15mm respectively and after that it is decreasing with slower rate. Hence it is concluded that, as external damping increases, maximum dynamic deflection λ_{max} is decreases with a decreasing rate.
5. For the base excitation amplitude Y=1mm, base excitation frequency ω =110 rad/s and at x location of 150mm from the clamped end the maximum dynamic deflection λ_{max} is obtained as 19.51mm. If base of this cantilever beam is fixed and external excitation force $f(x,t)$ is applied at x location equal to 150mm from the fixed end such that amplitude of force excitation F_0 is taken as 1N and frequency of base excitation ω is taken as 110 rad/s, the obtained λ_{max} value is 10.71mm. Hence it is observed that, as compared to equivalent forced excitation cantilever beam, the maximum dynamic deflection λ_{max}, is more in case of base excitation system.
6. For width b to thickness t ratio of 5, if b and t values taken in the MATLAB program as b=2.5mm and t=0.5mm, b=5mm and t=1mm, b=7.5mm and t=1.5mm, b=10mm and t=2mm, respective maximum dynamic deflection λ_{max} values are 3.87mm, 8.83mm, 18.43mm and 33.44mm. The same observation is for b/t ratio equal to 10 and 15. Hence it is concluded that, for the same value of b/t ratio if values of b and t are increased, the maximum dynamic deflection of the cantilever beam λ_{max} increases.

7. If thickness t is kept constant at 0.5mm, for b/t ratio of 5, 10 and 15 the maximum dynamic deflection λ_{max} is 3.87mm, 5.3mm and 6.27mm respectively. The same observation is for other thickness values. Hence it is concluded that, for the constant thickness value, maximum dynamic deflection λ_{max} of the cantilever beam increases with the increase in b/t ratio.
8. For the same length l=230mm, width b= 15mm and thickness t= 1.5mm of the cantilever beam and if other parameters kept constant i.e. base excitation amplitude Y=1mm, base excitation frequency ω =110 rad/s. At x location 150mm from the clamped end titanium alloy material Ti-6Al-4V has maximum dynamic deflection λ_{max} =19.51mm and for steel material AISI 1065 has maximum dynamic deflection λ_{max} =27.5mm.

REFERENCES

[1] Freundlich J. 2018. Transient vibrations of a fractional Kelvin-Voigt viscoelastic cantilever beam with a tip mass and subjected to a base excitation. Journal of Sound and Vibration 438 (2019) 99e115.
[2] Meesala V. 2018. Modeling and Analysis of A Cantilever Beam Tip Mass System. Blacksburg, Virginia.
[3] Sonawane A. and Talmale P. 2017. Modal Analysis of Single Rectangular Cantilever Plate by Mathematically, FEA and Experimental. International Research Journal of Engineering and Technology (IRJET).
[4] Skoblar A., Zigulic R., Braut S., Blazevic S. 2016. Dynamic Response to Harmonic Transverse Excitation of Cantilever Euler-Bernoulli Beam Carrying a Point Mass. Faculty of Engineering, University of Rijeka Vukovarska 58, 51000 Rijeka, Croatia.
[5] Pawar R. and Sawant S. 2015. Vibrational Analysis of Cracked Cantilever Beam Subjected to Harmonic Excitation with Nonlinear Parameters. International Journal of Science, Engineering and Technology Research (IJSETR), Volume 4, Issue 12.
[6] Kotambkar M. 2014. Effect of mass attachment on natural frequency of free-free beam: analytical, numerical and experimental investigation. Kotambkar, International Journal of Advanced Engineering Research and Studies E-ISSN2249–8974.
[7] Sun W, Liu Y., Li H., Pan D. 2013. Determination of the response destributions of cantilever beam under sinusoidal base excitation. Journal of Physics: Conference Series 448.
[8] Wu H., Tang L., Yang Y. and KiongSoh C. 2012. A novel two degrees of freedom piezoelectric energy harvester. Journal of Intelligent Material Systems and Structures.
[9] Velazquez I. 2007. Nonlinear Vibration of a Cantilever Beam. Thesis. Rochester Institute of Technology.
[10] Banks H. and Inman D. 1989. On damping mechanisms in beams. Institute for Computer Applications in Science and Engineering NASA Langley Research Center Hampton, Virginia 23665-5225.
[11] Meirovitch L. 2001. Fundamentals of Vibrations. Library of Congress Cataloging in Publication Data.
[12] Boresi A. 1985. Advanced Mechanics of Materials. Library of Congress Cataloging in Publication Data.
[13] Clough R. and Penzien J. 1993. Dynamics of Structures. Library of Congress Cataloging in Publication Data.
[14] Bhavikatti S. 1996. Strength of Materials. British Library Cataloguing in Publication Data.